

Synthesis and properties of amphotropic hydrogen bonded liquid crystalline (LC) poly(ester amide)s (PEA): effect of aromatic moieties on LC behavior

J.D. Sudha*, C.K.S. Pillai

Chemical Science Division, Polymer Section, Regional Research Laboratory (CSIR), Industrial Estate Post, Thiruvananthapuram 695019, Kerala, India

Received 7 March 2005; received in revised form 27 May 2005; accepted 28 May 2005

Available online 7 July 2005

Abstract

Twelve hydrogen bonded aromatic–aliphatic poly(ester amide)s differing in the structures of their aromatic moieties (isophthalic, terephthalic, 2,6-naphthyl and 4,4'-biphenyl moieties of the dicarboxylic acid and phenylene and xylylene moieties of the amido diol part) were prepared by the polycondensation of amido diols with acid chlorides of isophthalic acid, terephthalic acid, 2,6-naphthalic dicarboxylic acid and 4,4'-biphenyl dicarboxylic acid, respectively. The amido diols were prepared by the aminolysis of γ -butyrolactone with hexamethylene diamine, para phenylene diamine and para xylylenene diamine, respectively. The PEAs were characterised for elemental analysis, FTIR, ^{13}C NMR, TGA, DSC, POM, isothermal viscosity measurements and WAXD. Here we are presenting the effect of aromatic moieties on the thermotropic and lyotropic (amphotropic) properties of PEAs. These PEAs are essentially constituted of six types of structural entities, i.e. isophthalic, terephthalic, 2,6-naphthalic and 4,4'-biphenyl moieties containing dicarboxylic acid and the aliphatic, aromatic (phenylene and xylylene moieties) of the di-amide linkage of the amido diol part. The structure of the polymers even in the mesophase is dominated by hydrogen bond interaction between the adjacent chains and also inter plane mesogenic interaction between the rigid aromatic group. It was observed morphologically that the formation of different forms of nematic/smectic/columnar/spherulitic phases in PEAs are due to the delicate balance of self assembling through hetero intermolecular hydrogen bonded amide–amide and amide–ester networks and also inter-plane mesogenic interactions.

© 2005 Elsevier Ltd. All rights reserved.

Keywords: Amido diol; Hydrogen bonding; Liquid crystalline

1. Introduction

In recent years considerable attention has been devoted to LC materials formed by self assembling through a high degree of non covalent interactions like intermolecular hydrogen bonding, electron donor–acceptor interactions as well as by mesogenic interactions [1–16]. Intermolecular hydrogen bonding, chain stiffness and persistence length can vary with the structural moieties present in the polymer chain which can influence the nature and stability of the mesophase formed [16]. Amphotropic LC polymers are those, which can exhibit mesogenic behavior in concentrated solution (lyotropic behavior) as well as in the pure

form at elevated temperature (thermotropic behavior) and can form smectic or nematic depending upon their persistence length. Polyisocyanates and substituted carbohydrates of aliphatic or aralkyl side chains of appropriate length exhibited both thermotropic and lyotropic liquid crystallinity. In the case of polyisocyanate, the main chain extension and rigidity are mostly due to the *cis–trans* configuration of the adjoining amide bonds along the chain and in carbohydrate, the rigidity is due to the intermolecular hydrogen bonding. Para linked polyurethanes exhibited liquid crystallinity even in the absence of mesogenic groups [14] due to the rigidity arising from intermolecular hydrogen bonds among the urethane linkages (–NHCOO–). For main chain and side chain LC polymers, it was also revealed that orientation of the polymer chains is assisted by electron donor–acceptor interactions as well as mesogenic interactions resulting in nematic phase and highly ordered smectic phases [15].

* Corresponding author. Tel.: +91 471 2515316; fax: +91 471 2491712.
E-mail address: sudhajd2001@yahoo.co.in (J.D. Sudha).

Aromatic–aliphatic PEAs are well known to exhibit liquid crystalline properties mainly due to the intermolecular hydrogen bonding between amide–amide and amide–ester moieties [7–14]. We have shown earlier that amido diol is an important precursor for the synthesis of novel PEAs containing built-in di-amide linkage and that the extensive hydrogen bonding between the amide–amide and amide–ester moieties stabilizes the mesophase structures of the PEAs [7]. The rigidity due to the aromatic ring and the double bond character of carbonyl group coupled with extensive hydrogen bonding influence the ordering of PEAs causing LC behavior. It would be interesting, therefore, to investigate the influence of various aromatic entities differing in size and structure on the intermolecular interactions and LC phase transitions of this system.

In this communication, we present the synthesis and characterization of new high molecular weight PEAs prepared by the solution polycondensation of diamide containing aralkyl and alkyl diol with dicarboxylic acid of different aromatic structure. The thermotropic behavior of these polymers was studied using DSC, POM and XRD. The lyotropic phase transitions were studied by isothermal viscosity measurement in combination with POM. Intermolecular hydrogen bonding that influences the LC behavior was studied by variable temperature FTIR spectroscopy.

2. Experimental

2.1. Materials and methods

Bis(hydroxy butyramido) hexane (BHHH), bis(hydroxy butyramido)xylene (BHBX), 1,4-[bis(hydroxy butyramido) benzene] (BHBD), 2,6-naphthalene dicarboxylic acid, 4,4'-biphenyl dicarboxylic acid and isophthalic acid, terephthalic acid were obtained from Fluka and used as such. Thionyl chloride, triethyl amine (TEA), dimethyl formamide (DMF), *N*-methyl pyrrolidone (NMP) and *m*-cresol was purchased from E-Merck and purified as per the procedure given by Perrin et al. [17]. The inherent viscosities of the polymers were measured using Ubbelohde suspended level viscometer at 40 °C. The polymer concentration was 0.5 gm/dl in *m*-cresol. Melting point of the monomers and phase transitions were observed under Nikon Optiphot polarised light microscope equipped with Linkam THMS 600 heating stage connected to TP 92 temperature programmer. DSC scans were performed using DuPont DSC 2010 differential scanning calorimeter attached to thermal analyst 2100 data solution under nitrogen and TGA using DuPont 951 thermogravimetric analyser under air and nitrogen at a heating rate of 20 °C/min. Wide angle X-ray diffractograms were recorded on a Rigaku Mini flux X-ray diffractometer using nickel filtered Cu K_α radiation. Infra-red spectra were measured (KBr pellets {1–5 wt%}) using a Nicolet impact 400D FTIR spectrophotometer. KBr samples were heated in

an oven at 150 °C for 2 h and cooled from a desiccator. Blank FTIR spectrum was recorded using the dried KBr and samples were recorded using the same amount of KBr and keeping the same number of scans. Then the blank was subtracted from the sample spectra.

¹H NMR and ¹³C NMR spectra were recorded in trifluoroacetic acid with a Bruker 300 MHz FT NMR equipped with an ASPECT-3000 computer. The viscosities of the PEA solutions at different shear rates were measured with a Haake viscometer. Polymers were dissolved in *m*-cresol to produce a birefringent solution. Dissolution was achieved in two days with heating and agitation. Solutions of lower concentrations were prepared by subsequent dilution after completing all measurements at higher concentration.

2.2. Synthesis of monomers

2,6-Naphthalene dicarboxyloyl chloride, 4,4'-biphenyl-dicarboxyloyl chloride, isophthaloyl chloride and terephthaloyl chloride were prepared as per the procedure given by Sorensen and Campell [18]. The amido diols, bis(hydroxy butyramido) hexane (BHHH), bis(hydroxy butyramido)xylene (BHBX) and 1,4-[bis(hydroxy butyramido)phenylene] (BHBD) were prepared by the aminolysis of γ -butyrolactone, δ -valerolactone, ϵ -caprolactone using hexamethylene diamine, paraphenylene diamine and xylylene diamine, respectively, as per the procedure reported earlier [7,8].

2.3. Polymer synthesis

2.3.1. Poly[1,6-bis(4-isophthalate butyramido)]hexane (P1)

BHBH—2.80 g (0.1 mol) was taken in a perfectly dried three necked 100 ml round bottom flask with a magnetic stirrer and was fitted with calcium chloride guard tube and a nitrogen purging tube. 250 ml of perfectly dried NMP was added to the amido diol and stirred well to dissolve it. Nitrogen was then purged through the system to remove all moisture and also to provide an inert atmosphere. It was then placed in an ice-cold bath (0–5 °C). 1 g of TEA (0.01 mol) was added followed by 2.03 g (0.01 mol) isophthaloyl chloride. The reaction was continued with stirring under nitrogen atmosphere for 3 h at room temperature. The contents were then poured into methanol and was filtered and washed several times with hot sodium bicarbonate solution followed by washing with methanol several times. This was then dried at 80 °C and then powdered and further purification was effected by soxhlet extraction in acetone/isopropanol mixture for 16 h. It was then dried under vacuum at 80 °C for 4–6 h. Yield=75%. Colour and appearance—colourless powdery material. Inherent viscosity 0.51 dl/g. FTIR (KBr) cm⁻¹: 3311 and 3081 (both NH stretching of the secondary amide linkage); 2936 and 2870 (CH stretching of CH₂); 1637 and 1553

(secondary amide I and secondary amide II band); 1712 (C=O stretching of the ester). ^{13}C NMR δ (ppm): 184 (–NH–C=O–); 172 (–COO). Elem. Anal. Calcd for $(\text{C}_{22}\text{H}_{30}\text{N}_2\text{O}_6)_n$: %: C, 63.14; H 7.23; N=6.69. Found %: C, 63.10; H, 7.18; N, 6.6.

2.3.2. Synthesis of poly[1,4-bis(4-isophthalate butyramido)]xylylene (P2)

PBIBX was synthesised from BHBX 3.08 g (0.01 mol) and isophthaloyl chloride 2.03 g (0.01 mol) and the procedure is similar to the one described above. Yield 70%; colour and appearance—colourless powder; inherent viscosity 0.52 dl/g. FTIR (KBr) cm^{-1} : 3277, 3058 (NH stretching of secondary amide linkage); 2939 and 2859 (both CH stretching of CH_2); 1639 (amide I band); 1540 (secondary amide II band); 1719 (C=O stretching vibration of the ester). ^{13}C NMR δ (ppm). 184 (–NH–C=O–); 172 (COO). Elem. Anal. Calcd for $(\text{C}_{24}\text{H}_{26}\text{N}_2\text{O}_6)_n$: %: C, 65.89; H, 5.76; N, 6.40. Observed: %: C, 65.79; H, 5.75; N, 6.45.

2.3.3. Synthesis of poly[1,4-bis(4-isophthalate butyramido)]phenylene (P3)

PBIBB was synthesised from isophthaloyl chloride 2.03 g (0.01 mol) and BHBB 2.80 g (0.01 mol). A similar procedure as above was adopted. Yield 68%; colour and appearance—colourless powder; inherent viscosity 0.68 dl/g. FTIR (KBr) cm^{-1} 3329 and 3071 (NH stretching vibrations of secondary amide I linkage); 2985 and 2879 (CH stretching of $-\text{CH}_2$), 1636 (secondary amide band); 1537 (secondary amide II band); 1716 (C=O stretching of the ester group). ^{13}C NMR δ (ppm): 184 (–NH–C=O–); 172 (–COO). Elem. Anal. Calcd for $(\text{C}_{22}\text{H}_{22}\text{N}_2\text{O}_6)_n$: %: C, 64.38; H, 5.4; N, 6.83. Observed %: C, 64.39; H, 5.45; N, 6.80.

2.3.4. Synthesis of poly[1,4-bis(4-2,6-naphthalene dicarboxylate butyramido)]hexane (P4)

PBNBH was synthesised from 2,6-naphthalene dicarboxyloyl chloride 2.53 g (0.01 mol) and BHBH 2.82 g (0.01 mol). A similar procedure as described in earlier was used.

Yield 68%; colour and appearance—yellow powdery material; inherent viscosity 0.73 dl/g. FTIR (KBr) cm^{-1} : 3332 (NH stretching of secondary amide linkage); 2943 and 2870 (CH stretching vibrations due to $-\text{CH}_2$ group); 1716 (C=O stretching of the ester); 1640 (amide I band and amide II band). ^{13}C NMR δ (ppm): 179 (–CONH–); 170 (–O–CO–). Elem. Anal. Calcd for $(\text{C}_{22}\text{H}_{32}\text{N}_2\text{O}_6)_n$: %: C, 66.65; H, 6.88; N, 5.98. Observed %: C, 66.59; H, 6.80; N, 5.90.

2.3.5. Synthesis of poly[1,4-bis(4-2,6-naphthalene dicarboxylate butyramide)]xylylene (P5)

PBNBX was synthesised from 2,6-naphthalene dicarboxyloyl chloride 2.53 g (0.01 mol) and BHBX 3.08 g (0.01 mol). A similar procedure as described in the case of 1

was used. Yield 72%; colour and appearance—yellow powdery material; inherent viscosity 0.65 dl/g. FTIR (KBr) cm^{-1} : 3396 and 3018 (NH stretching vibration of secondary amide linkage); 2948 and 2870 (CH stretching of the CH_2 group); 1721 (C=O stretching of the ester group); 1640 (secondary amide I band), 1537 cm^{-1} (secondary amide II band). ^{13}C NMR δ (ppm): 78 (–CONH–); 170 (–O–CO–). Elem. Anal. Calcd for $(\text{C}_{28}\text{H}_{28}\text{N}_2\text{O}_6)_n$: %: C, 68.84; H, 5.78; N, 5.73. Observed %: C, 68.79; H, 5.80; N, 5.70.

2.3.6. Synthesis of poly[1,4-bis(4-2,6-naphthalene dicarboxylate butyramido)]benzene (P6)

PBNDB was synthesised from 2,6-naphthalene dicarboxyloyl chloride 2.53 g (0.01 mol) and BHBB 2.80 g (0.01 mol). A similar procedure as described for 1 was used.

Yield 70%; colour and appearance—yellow powdery material; inherent viscosity 0.65 dl/g. FTIR (KBr) cm^{-1} : 3429, 3071 and 3012 (NH stretching of secondary amide linkage); 2985, 2879 (–CH vibrations due to $-\text{CH}_2$ group); 1715 (C=O stretching of the ester group); 1633 (secondary amide I band); 1513 (secondary amide II band). ^{13}C NMR δ (ppm): 179 (–CONH–); 170 (–O–CO–). Elem. Anal. Calcd for $(\text{C}_{26}\text{H}_{24}\text{N}_2\text{O}_6)_n$: %: C, 67.82; H, 5.25; N, 6.08. Observed %: C, 67.80; H, 5.20; N, 6.10.

2.3.7. Synthesis of poly[1,6-bis(4-biphenyl dicarboxylate butyramido)]hexane (P7)

PBBBH was prepared from 4,4'-biphenyl dicarboxyloyl chloride 2.79 g (0.01 mol) and BHBH 2.82 g (0.01 mol) were taken. A similar procedure as described in 1 was used.

Yield 72%; colour and appearance—colourless. Inherent viscosity 0.81 dl/g. FTIR (KBr) cm^{-1} 3322 (NH stretching of secondary amide linkage); 2943 and 2870 (CH stretching vibrations due to $-\text{CH}_2$ group); 1716 (C=O stretching of the ester); 1640 (amide I band); 1537 (amide II band). ^{13}C NMR δ (ppm): 177 (–CONH–); 169 (–O–CO–). Elem. Anal. Calcd for $(\text{C}_{28}\text{H}_{28}\text{N}_2\text{O}_6)_n$: %: C, 68.84; H, 5.78; N, 5.73. Observed %: C, 68.79; H, 5.80; N, 5.70.

2.3.8. Synthesis of poly[1,4-bis(4-4'-biphenyl dicarboxylate butyramido)]xylylene (P8)

PBBBX was synthesised from 4,4'-biphenyl dicarboxyloyl chloride 2.79 g (0.01 mol) and BHBX 3.09 g (0.01 mol) were taken. A similar procedure as described in 1 was used.

Yield 72%; colour and appearance—colourless powdery material; inherent viscosity 0.69 dl/g. N, 5.70. FTIR (KBr) cm^{-1} : 3277 and 3058 (–NH stretching of secondary amide linkage); 2939 and 2858 (CH stretching vibrations due to CH_2 group); 1720 (C=O stretching of the ester group); 1633 (secondary amide I band); 1537 (secondary amide II band). ^{13}C NMR δ (ppm): 179 (–CONH–); 171 (–O–CO–). Elem. Anal. Calcd for $(\text{C}_{28}\text{H}_{28}\text{N}_2\text{O}_6)_n$: %: C, 68.84; H, 5.78; N=5.73. Observed %: C, 68.79; H, 5.80.

2.3.9. Synthesis of poly[bis(4,4'-biphenyl dicarboxylate butyramido)] phenylene (P9)

PBBBB was synthesised from 4,4'-biphenyl dicarboxyl chloride 2.79 g (0.01 mol) and BHBB 2.80 g (0.01 mol). A similar procedure as described for I was used.

Yield-70%. Colour and appearance—colourless powdery material. Inherent viscosity -0.75 dl/g. FTIR (KBr) cm^{-1} : 3436, 3058 and 3012 ($-\text{NH}$ stretching of the secondary amide linkage); 2965 and 2840 (CH stretching vibrations due to $-\text{CH}_2$ group); 1715 ($\text{C}=\text{O}$ stretching vibration due to ester); 1633 (secondary amide I band); 1543 (secondary amide II band). ^{13}C NMR δ (ppm): 179 ($-\text{CONH}-$); 171 ($-\text{O}-\text{CO}$). Elem. Anal. Calcd for $(\text{C}_{28}\text{H}_{28}\text{N}_2\text{O}_6)_n$ %: C, 69.12; H, 5.40; N, 5.76. Observed %: C, 69.09; H, 5.40; N, 5.66.

2.3.10. Synthesis of poly [1,6 bis(4-terephthalate butyramido)]hexane (P10)

P10 was synthesized as reported earlier [7].

2.3.11. Synthesis of poly [1,4 bis(4-terephthalate butyramido)]phenylene (P11)

P11 was synthesized as reported earlier [8].

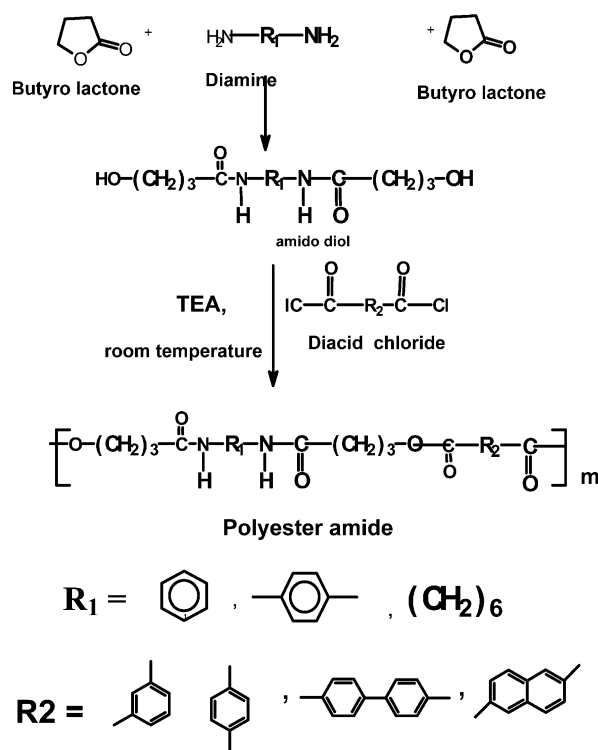
2.3.12. Synthesis of poly [1,4 bis(4-terephthalate butyramido)]xylylene (P12)

P12 was synthesized as reported earlier [8].

3. Results and discussion

Twelve PEAs were prepared by solution polycondensation [19] between the diacid chlorides of structurally different aromatic moieties (isophthalic, terephthalic, 2,6-naphthyl and 4-biphenyl) and the amido diols BHHH, BHBB and BHBD using TEA as acid acceptor in NMP as per Scheme 1. The experimental details are listed in Table 1. The polymers were obtained in comparatively good yield. Solubility studies of PEAs were performed with 0.1 gm of polymer in 10 ml of solvents having different polarity and the results are given in Table 2. Most of the PEAs were soluble in highly polar solvents such as *m*-cresol, NMP, conc. H_2SO_4 and were found to be insoluble in tetrahydrofuran, chloroform etc. The extent of solubility of PEAs is in the order, isophthaloyl > terephthaloyl > biphenyl > naphthyl. Based on the amido diol moiety, the solubility decreases in the order hexamethylene > *p*-xylylene > *p*-phenylene. Inherent viscosities (I.V) of the PEAs measured in *m*-cresol at 50 °C (0.2 g/dl) were in the range 0.7–0.9 dl/g. The PEAs having 2,6-naphthalene and biphenyl groups were found to give higher inherent viscosity possibly due to the presence of bulky groups [20] than those containing isophthaloyl and terephthaloyl groups (Table 1).

The formation of the PEAs was confirmed by elemental analysis, FTIR, ^1H NMR and ^{13}C NMR. FTIR spectra of all

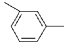
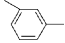

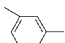
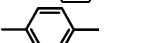
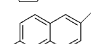
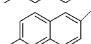

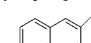
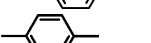
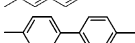
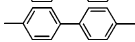

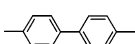
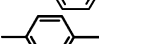
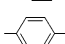
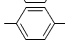

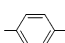
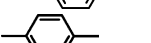


Scheme 1. Synthesis of poly(ester amide)s.

PEAs showed a broad dominant band in the range 3310 and 3067 cm^{-1} and the peak position of this band changes slightly with the change in the structure of PEAs. This broad band is characteristic of hydrogen-bonded trans form of the amide group [21]. A weak shoulder at about 3426 cm^{-1} , characteristic of non-hydrogen-bonded, free N–H stretching was exhibited by most of these PEAs. This is consistent with the observation made by Coleman et al. [20]. The structures of the PEAs were further confirmed by ^1H NMR (acetone d_6 , 300 MHz) and ^{13}C NMR (acetone d_6 , 75 MHz). In ^1H NMR, the peak at δ (ppm) = 7.9–8 ($-\text{Ar}-$), 4.5–4.7 ($-\text{COCH}_2-$); 3.9 ($-\text{C}-\text{NH}-\text{CH}_2$); 1.3–2.1 ($(\text{CH}_2)_m$). In ^{13}C NMR, the resonance signals at δ (ppm) = 180, 172–174, 139, 65.3, 29.6, 46, 38–18.2 correspond to ($-\text{CONH}-$), ($-\text{COO}-$), ($-\text{Ar}-$), ($\text{Ar}-\text{C}=\text{O}$); ($-\text{CH}_2\text{O}-$); ($-\text{CONHCH}_2\text{CH}_2-$), ($-\text{CH}_2\text{NH}-$), ($-\text{COCH}_2\text{CH}_2-$), respectively.

Typical FTIR spectra of LCPEAs containing isophthalic, naphthalic, biphenylic and terephthalic moieties are shown in Fig. 1. It can be observed that in general, there exists a remarkable similarity among the room temperature spectra, except the bands associated with the aliphatic and aromatic C–H bands which changes essentially according to the number of aromatic and methylene groups. FTIR spectra of the most of the prepared polymers showed broad band with overlaying shoulders in the region of 3300–3400 cm^{-1} indicating that in PEAs, more type of hydrogen bonds with different bond distances for N–H groups are formed. [23]. The absorption band in the region 1800–900 cm^{-1} consists of ester carbonyl and amide carbonyl region with multiple bands. An intense band in the region 1720 cm^{-1}

Table 1
Experimental details of synthesis of polyester amide

Sample	Structure of the diacid	Amido diol $\text{OH}(\text{CH}_2)_3\text{COHNRNHCO}(\text{CH}_2)_3\text{OH R}$	Yield %	Inherent viscosity (dl/g)	Colour and appearance
P1		$(\text{CH}_2)_6$	70	0.75	Colourless powder
P2			72	0.88	Colourless powder
P3			68	0.78	Colourless powder
P4		$(\text{CH}_2)_6$	72	0.81	Colourless powder
P5			70	0.86	Yellow powder
P6			59	0.79	Colourless powder
P7		$(\text{CH}_2)_6$	61	0.68	Colourless powder
P8			65	0.67	Colourless powder
P9			69	0.64	Colourless powder
P10		$(\text{CH}_2)_6$	71	0.71	Colourless powder
P11			74	0.75	Colourless powder
P12			75	0.80	Yellow powder

corresponds to the ester carbonyl attached to aromatic ring and its intensity and frequency varied with the type of aromatic ring. The peak at 1633 and 1550 cm^{-1} corresponds to the amide I and amide II band, respectively. The peak at 935 and 1145 cm^{-1} have been identified as crystalline and amorphous region, respectively, as assigned by Haberkorn et al. [24] for C–O twist (1145 cm^{-1}) and C–CO stretch (935.5 cm^{-1}). To elucidate the contribution of hydrogen bonds to the thermotropic liquid crystallinity, FTIR spectra of typical PEA (P8) were measured at different temperatures like 30°C , 160°C , and after cooling from isotropisation temperature, 240°C . The importance of hydrogen bond interaction between N–H for the formation of supramolecular columnar mesophases was reviewed by Uwe Beginn [25]. Hydrogen bonds have a major impact on the vibrational properties of hydrogen-bonded groups. So

infra red spectroscopy is well suited for the study of the influence of hydrogen bonding during mesophase formation and isotropisation [26,27]. Fig. 2(a)–(c) summarise the changes in the vibration spectra connected with hydrogen bonding in the region $3000\text{--}3400\text{ cm}^{-1}$ of P8 at room temperature, mesophase transition and also after cooling from the melt for P6. At 30°C , the broad band in the region $3500\text{--}3300\text{ cm}^{-1}$ with overlaying shoulder indicated the presence of different types of hydrogen bonds with different bond distances for N–H groups. Upon heating at 170°C , the band changes its shape and a sharp peak at 3310 cm^{-1} was observed corresponding to the N–H stretching of hydrogen-bonded trans form of the amide group [28]. The transition from mesophase to the isotropic phase is accompanied by the substantial decrease of hydrogen bonds. Thus, the rigidity due to the hydrogen bonding is responsible for the

Table 2
Solubility studies of PEAs

Sample	Conc. sulphuric acid	<i>m</i> -Cresol	<i>N</i> -Methyl pyrrolidone	DMAC	DMF	THF
P1	+	+	±	±	±	–
P2	±	±	±	±	–	–
P3	+	+	±	±	–	–
P4	+	+	+	+	+	–
P5	+	±	±	±	±	–
P6	+	±	±	±	±	–
P7	±	±	±	–	–	–
P8	+	+	±	±	±	–
P9	±	±	±	–	–	–
P10	+	±	±	±	±	–
P11	+	+	±	±	–	–
P12	±	±	±	±	–	–

Solubility checked with 0.1 g polymer/10 ml of solvent (+) soluble; (±) soluble on heating; (–) insoluble.

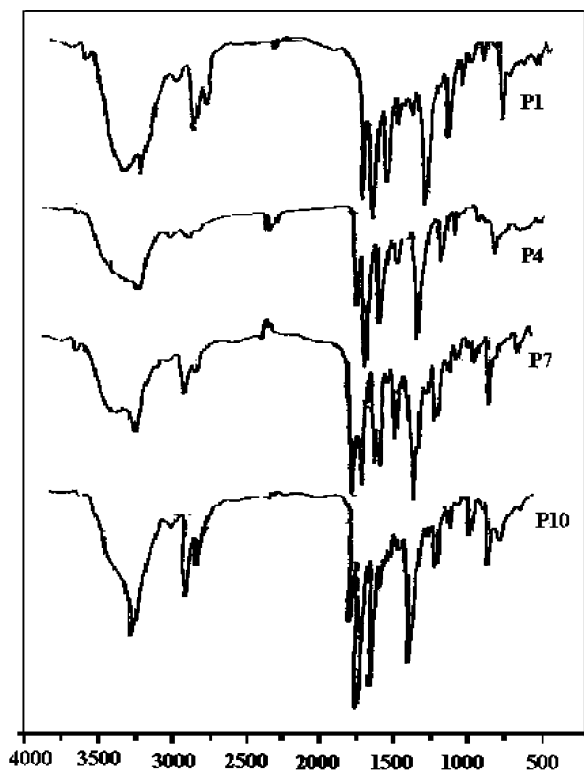


Fig. 1. FTIR (KBr) spectra of LCPEAs containing isophthalene (P1), naphthalene (P4) biphenylene (P7), terephthalene (P10) moieties.

liquid crystallinity for these PEAs and the stable smectic LC phase is formed by self organization through the formation of hetero intermolecular hydrogen bonded networks. The ester segments can exist in more than one conformational form and hence it exhibits the transition from one smectic texture to another of the same texture. PEA contains two different types of hydrogen bonds i.e. amide–amide and amide–ester bonds and at elevated temperature amide–ester hydrogen bonds are more stable than amide–amide bonds. The structure of the polymers even in the mesophase is dominated by hydrogen bonds among the amide–ester and amide–amide groups in the adjacent chains. When the KBr pellet was further heated to melting and then cooled to room temperature the corresponding spectra showed two well defined sharp peaks confirming that during heating and cooling hydrogen bonding is retained. Fig. 2 (a)–(c) shows the vibrational changes taking place in the region 1720–900 cm^{-1} in P6 at room temperature, at the mesophase transition temperature and also after cooling from the melt. This region will give the changes in the vibrational spectra of ester carbonyl and amide carbonyl and the hydrogen bond interaction between the ester amide and amide–amide groups. An intense peak observed at 1715 cm^{-1} at room temperature is typical for aromatic ester carbonyl groups and the band at 1633 and 1550 cm^{-1} corresponds to the carbonyl peak of amide I band and amide II band, respectively. The intensity and frequency of the ester carbonyl and amide carbonyl band changed substantially at

the mesophase and isotropisation temperature. In a similar fashion, the amide I band (1633 cm^{-1}) and amide II band (1540 cm^{-1}) broadened and shifted to larger wave numbers. The nature of hydrogen bonding in PEAs was studied by Bozena Kaczmarczyk et al. [29]. The decrease in the band at 1717 cm^{-1} , with simultaneous increase in the bands at 1648 and 1553 cm^{-1} in the FTIR spectra of Polymer P8 during heating, confirms the fact that on heating, some of the amide–ester hydrogen bonds change into amide–amide hydrogen bonds. The band at 1275 cm^{-1} can be assigned to the deformation vibration of the amide–amide bonded N–H (amide III) band. This implies the hydrogen bonding of ester carbonyl with N–hydrogen of the amide linkage. The existence of different mesophases is due to the formation of different types of hydrogen bonded and non-bonded structures. The peak positions of the ester carbonyl at 1715 cm^{-1} and amide carbonyl at 1634 cm^{-1} peaks were observed at lower frequencies than expected for the free ester and amide peaks. In PEAs, the band at 1260 cm^{-1} appeared only as shoulder and it partly overlaps with the band at 1275 cm^{-1} , characteristic of esters. The band at 1260 cm^{-1} can be assigned to the deformation vibration of the amide–amide bonded N–H (amide III band). Above 170 $^{\circ}\text{C}$, the band at 1260 cm^{-1} gradually decreased and that at 230 $^{\circ}\text{C}$ appeared only as a shoulder. After cooling the sample, the band at 1260 cm^{-1} had a slight diminution in intensity. During heating, a significant diminution occurred for the bands at 1633 cm^{-1} and that at 1712 cm^{-1} with a concomitant increase in the bands at 1660 and 1540 cm^{-1} .

Taking into account the results of FTIR analysis and liquid crystallinity observation, it can be assumed that PEAs have LC orientation both by mesogenic interaction [29] and by hydrogen bonding between the amide–amide and amide–ester. The mesogenic interaction is explained as inter-plane interaction and hydrogen bonding is due to in-plane interaction between the adjacent chains as shown in the Scheme 2.

Thermal and phase transitions of PEAs were studied using polarised optical microscopy in combination with differential scanning calorimetry. These polymers are essentially constituted of six types of structural entities i.e. isophthalic, terephthalic, 2,6-naphthyl and 4-biphenyl moieties of the dicarboxylic acid and the aliphatic, aromatic (benzene and xylylene moieties) and the di-amide linkage of the amido diol part. Thus, the changes in thermal and phase behavior could be expected mainly from contributions from the aromatic moieties as the di-amide linkage and the aliphatic moieties are common to all polymers.

The first heating DSC scans of P10, P1, P4, P3, P8, P2, P5, P9 are given in Fig. 3. The detailed DSC and POM studies on thermal and phase transitions are summarized in Table 3. As reported earlier, P10 having terephthalic moiety from the dicarboxylic acid and the aliphatic segment from the amido diol showed the typical threaded texture of nematic liquid crystal. This has been explained as due to the

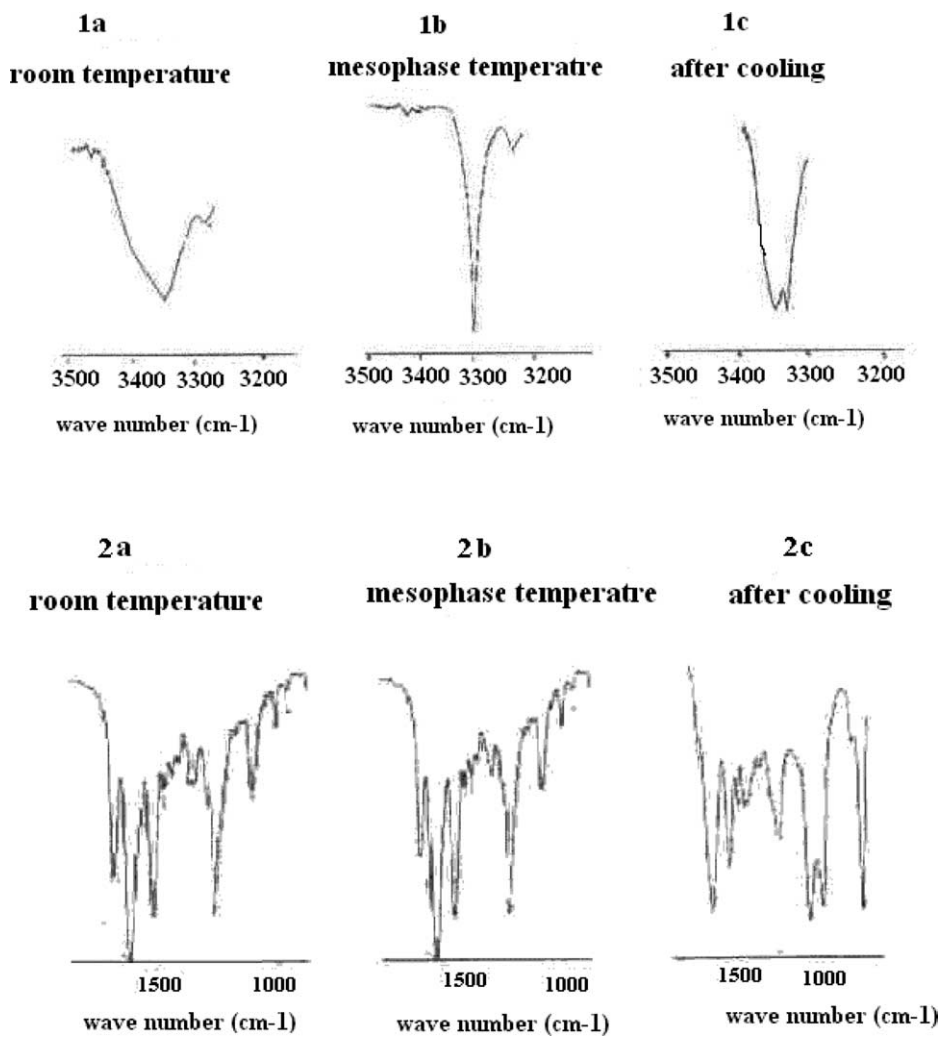
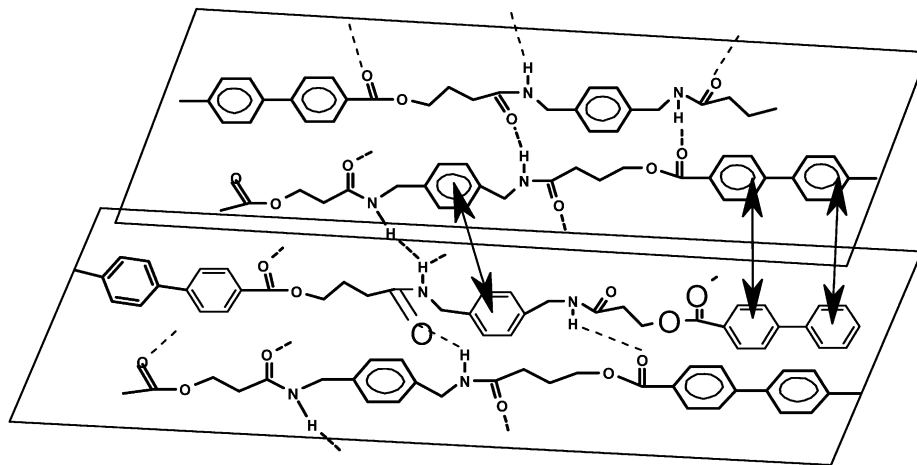


Fig. 2. FTIR spectra of P8 at $3400\text{--}3200\text{ cm}^{-1}$, (1a) at room temperature, (1b) at $160\text{ }^{\circ}\text{C}$, (1c) on cooling from the melt. FTIR spectra of P8 at $1720\text{--}900\text{ cm}^{-1}$ for P8 at (2a) room temperature, (2b) at the mesophase transition temperature and (2c) after cooling from the melt.



Scheme 2. Illustration of in-plane inter molecular hydrogen bonding interaction between the adjacent chains and inter-plane mesogenic interaction among the polymer chains in P8.

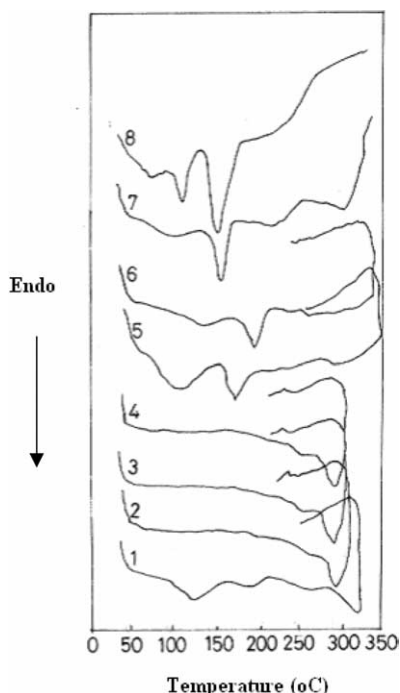


Fig. 3. DSC scans of (1) P10, (2) P1, (3) P4, (4) P3, (5) P8, (6) P2 (7) P5, (8) P9.

stabilisation of the LC phase by extended hydrogen bonding from the di-amide linkage. In contrast, P12 containing a benzene moiety from the amido diol part did not exhibit any LC phase instead, it showed a spherulitic texture. This can be explained as due to the direct attachment of the phenyl group with two amide groups, and the amide carbonyl

double bonds which are trans to each other forcing the benzene ring out of plane so that the rigidity (persistence length) will be insufficient for bringing LC phase. Similar observations have been reported by Krigbaum et al. [30]. The decrease in persistence length can be offset by replacing benzene ring with xylylene unit, which allows the two-amide carbonyl double bonds to be cis to each other, and the conjugation thus obtained gives sufficient rigidity for inducing mesophase in polymer P11. A structurally similar situation has been encountered when the terephthaloyl moiety was replaced by the naphthalene moiety with polymer P4 showing worm like threaded texture and P6 not exhibiting any mesophase textures while P5 exhibited grainy smectic textures. While the polymer P7 exhibited a threaded nematic texture at 140 °C, polymer P9 that contains biphenylene group lost liquid crystallinity and gave spherulitic structures. The polymer P8 again with biphenylene group, but xylylene moiety in the amido diol part showed mesophase structure at 180 °C as expected. The DSC scans of P9 in Fig. 3 exhibited abrupt changes in the DSC. Similar observations have been reported for thermotropic LC polyesters containing biphenylene moieties [31]. Bhowmic et al. [32] reported that the abrupt endotherms observed in DSC scan of the biphenyl containing PEAs can be due to the unsymmetrical structure of the biphenyl moiety and will undergo the change in the dihedral angle which serves a dual role in suppression of T_m and crystallinity of this polymer. The DSC traces do not show any T_m for the polymers containing isophthaloyl units. This can be attributed to the decrease in chain stiffness due to the bent structure of the isophthaloyl units [33]. It can be seen

Table 3
Thermal and phase transitions of PEAs

Sample	Structure of the diacid	Amido diol $\text{OH}(\text{CH}_2)_3\text{COHNRNHCO}(\text{CH}_2)_3\text{OH}$ R	T_c (°C)	T_m (°C)	T_{m-1} (°C)	Nature of texture
P1		$(\text{CH}_2)_6$	100	180	220	Spherulites
P2			95	–	335	Spherulites
P3			100	175	230	Spherulites
P4		$(\text{CH}_2)_6$	75	160	220	Grainy/smectic texture
P5			–	–	280	Spherulites/maltese cross
P6			–	180	260	Spherulites
P7		$(\text{CH}_2)_6$	50	105	245	Wormlike thread/columnar
P8			90	152	275	Threaded nematic
P9			90	152	275	Spherulites
P10		$(\text{CH}_2)_6$	82	140	195	Threaded nematic
P11			80	–	220	Smectic/batonnet/
P12			80	160	220	Spherulites

from Table 3 that the mesophase transition temperature is in the order, isophthaloyl < naphthyl < terephthaloyl < biphenyl. The higher T_{K-N} value of 2,6-naphthalene moiety containing PEA, compared to that of terephthaloyl moiety containing PEA can be related to the offset structure of the 2,6-ester linkage of naphthalene dicarboxylate as compared to the collinear 1,4-linkage of terephthalic acid and is supported by the work carried several research groups [34,35].

It has been shown earlier that the structure of the polymers even in the mesophase is dominated by hydrogen bonds between the amide–ester and amide–amide groups in the adjacent chains. In contrast to the earlier observation of a dominant role for hydrogen bonding in the stabilization of the mesophase, the phase behavior of the polymers indicates that the structure of the aromatic moieties play a significant role in the induction of the LC phase. Fig. 4 depicts the POM photographs of different LC PEAs. On the basis of numerous reports, it can be concluded that the induction and stabilization of liquid crystalline phases of the LCPs depend strongly on the chemical structure and thermal history [36]. Fig. 4(1) depicts the snowflake like spherulites of naphthalene containing PEAs (P5), when cooled from the nematic melt. Fig. 4(2) shows typical smectic texture exhibited by xylylene-containing LC PEA (P2) (2). Fig. 4(3) is the grainy texture exhibited by the P10 when cooled from the nematic melt at 170 °C. Worm-like threaded textures were exhibited by polymers P1, P7, P9, P8, P10 and P4. A typical worm-like threaded nematic texture exhibited by P8 is shown in Fig. 4(4). Rod-like texture typical of smectic C/batonet texture was exhibited by polymers P4, P11 and P12, when cooled from the LC phase. A typical batonet texture (P4) is shown in Fig. 4(5). When polymer P11 is cooled from the melt, a structure similar to spherulitic textures with a radial fibrillar growth and clear maltese crossed extinction pattern/columnar phase was obtained as shown in Fig. 4(f). The occurrence of the different types of mesophases is due to the different ways of ordering due to the self-assembling through different types of hetero intermolecular hydrogen bonding among amide–amide and amide–ester net works [37] and also due to the inter plane mesogenic interactions (Scheme 2).

Lytotropic behavior of PEAs induced by hydrogen bonding effect was studied by isothermal viscosity measurements at different shear rates in combination with POM as reported earlier by us [10]. In the lyotropic system, the dissolution and subsequent appearance of liquid crystallinity take place in solvents that can break up the inter chain hydrogen bonds present in the polymer and replace them by polymer-solvent hydrogen bonds. When these chains are connected by polymer–polymer inter chain hydrogen bonds, liquid crystallinity ceases to exist and the polymer separates out into crystalline, semicrystalline or amorphous state. The polymer was based on terephthalate aromatic moiety and hexamethylene aliphatic spacer. Typical viscosity vs. concentration curve of polymer P8 in *m*-cresol at 40 °C is

as shown in Fig. 5. As the concentration increases, more and more molecules align and come close together due to extensive hydrogen bonding with a proportional increase in viscosity. After a particular concentration, the viscosity decreases abruptly and the molecules are in the completely ordered state. The sample under polarized optical microscope exhibited a completely birefringent anisotropic phase. Under shear forces, the hydrogen bonding can be broken allowing the system to slip past one another at a faster rate. Hence, viscosity of the lyotropic solution decreases with increase in shear rate. The effects of polarity of solvent, shear rate and also polydispersity on the threshold concentration were investigated and reported earlier for aliphatic dominated PEAs [10]. Below the critical concentration, polymer P8 exhibited anisotropic inclusion in isotropic phase (Fig. 5). A fully anisotropic phase above the threshold concentration gave typical nematic threaded texture under POM (Fig. 5). The critical and threshold concentrations for P8 were found to be 25 and 30%, respectively. Thus, the rigidity of the hydrogen bonded sheets due to the inter chain hydrogen bonding interaction between the chains, and inter-plane mesogenic interaction are together responsible for the rigidity and ordering in lyotropic phase behaviour in LCPEAs. The anisotropy of the lamellae composed layers of hydrogen-bonded sheets is the reasons for the lyotropic LC behavior exhibited by these PEAs.

Thermal stabilities of the PEAs were studied by TG measurements by heating the sample at a rate of 20 °C/min in nitrogen and air. The thermal stability in nitrogen atmosphere is greater than that in air. Detailed experimental results are given in Table 4. A typical TG/DTG curve of P8 exhibited two to three decomposition maxima as shown in Fig. 6. The first decomposition is due to the ester group and is confirmed by the vanishing of the peak at 1720 cm^{-1} (CO stretching of the ester) in FTIR spectra. The second decomposition is due to the amide linkage. Table 4 shows that the thermal stability of the PEAs is in the order isophthaloyl < terephthaloyl < naphthyl < biphenyl. The enhanced thermal stabilities of polymers containing biphenyl and 2,6-naphthyl moieties are naturally due to the rigid benzenoid rings, which stiffen the chains and raise pyrrolic decomposition temperature [36]. For similar reasons, the polymer containing isophthalic group having lower stiffness exhibits inferior thermal stability [37]. The percentage of char formation is greater for biphenyl unit and naphthyl unit.

Crystallinity of PEAs was studied using wide-angle X-ray diffractogram. Typical WAXD diagrams of polymers P1, P2, P3, P4, P5, P6, P7 and P8, respectively, are given in Fig. 7. Several sharp, well-defined peaks in the diffractogram of all PEAs are indicative of the formation of crystalline regions in the polymer. The sharp peak around $2\theta=20^\circ$ corresponds to a d-spacing of $\sim 4.5 \text{ \AA}$, equal to the length of the repeating [38] chain. This observation confirms that there is a local correlation in the

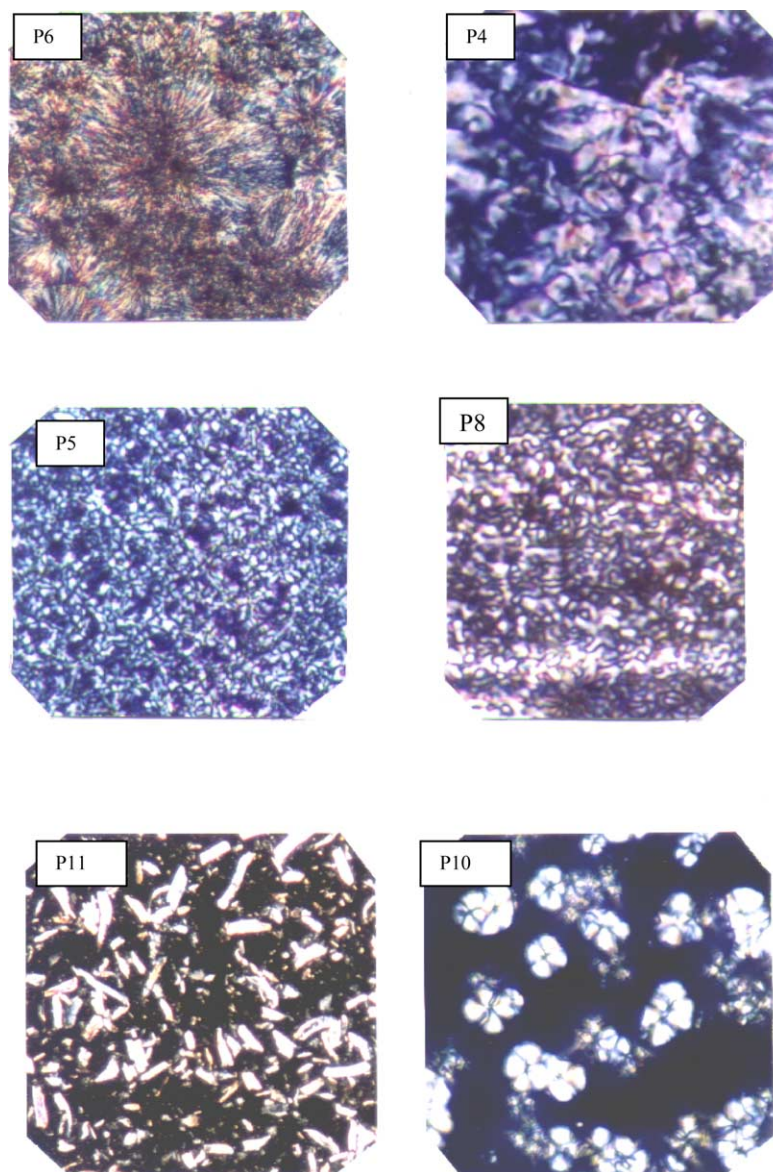


Fig. 4. The POM micrographs of (1) snow flake like spherulites (P5), (2) smectic texture (P2), (3) Grainy texture (P10), (4) worm like threaded texture (P8), (5) battonnet structure (P4), (6) columnar phase (P11).

Table 4
Thermal stability studies of PEAs

Polymer	T_5	T_{50}	T_{dmax1}	T_{dmax2}	Wt_{max1}	$Wt_{max2(C)}$
P1	295	430	336	430.9	75.75	51
P2	248	346	332	405.7	95.75	40
P3	341	465	383	485.7	69.5	63
P4	320	479	382	482	80.2	60
P5	290	410	344	440	85	57
P6	245	346	328	376	84	51
P7	315	400	387	490	86	67
P8	310	450	363	487	82	58
P9	319	436	353	480	74.5	57
P10	250	400	349	412.7	74.3	50
P11	330	490	385	470	80	62
P12	325	470	388	485	852	68

T_5 , T_{50} , T_{dmax1} and T_{dmax2} correspond to the temperatures in °C at which 5, 50% mass-loss occur, first maximum decomposition temperature and second maximum decomposition temperature appear.

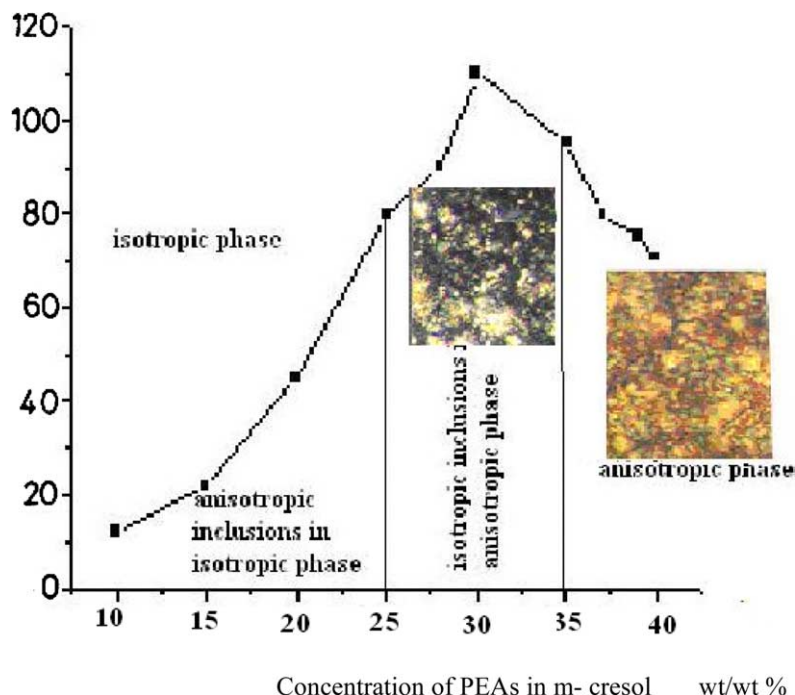


Fig. 5. Concentration vs. viscosity curve of P8 in meta cresol at 40 °C along with corresponding POM micrographs (a) anisotropic inclusion in isotropic phase (at low concentration) and (b) fully anisotropic nematic phase.

lateral arrangement of molecules. Percentage of crystallinity of the polymers was calculated according to the method reported by Tadkaro [39] by measuring the ratio of the area of the contribution of the crystalline part to the amorphous part and is given in Table 5. The lower percentage of crystallinity of IPA-containing PEA can be ascribed to the presence of non-linear *m*-phenylene units, which will disrupt the lateral interactions in the solid state. Similar observations have been reported out by Rubig et al. [40] for isophthalate containing LC polyesters. The WAXD pattern of polymer P11 that contains biphenyl unit showed *d*-spacing 19.3 Å, indicating that biphenyl moieties are nearly parallel and the presence of strong aromatic interactions promoting LC phase. This is reminiscent of the work carried out by several investigators for biphenyl containing polyesters

[41–43]. The lower crystallinity of PEAs containing NDA in contrast with TPA, is due to the offset structure of 2,6 ester linkage. This result is consistent with the observation of Calundann et al. [44,45] for naphthalene-containing copolyesters and terpolyesters.

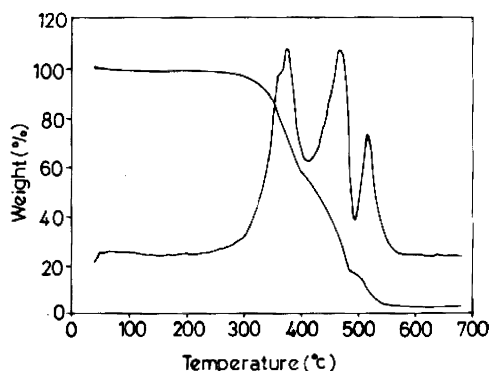


Fig. 6. TGA and DTG curve of P8 in N₂, heating rate 20 °C/min.

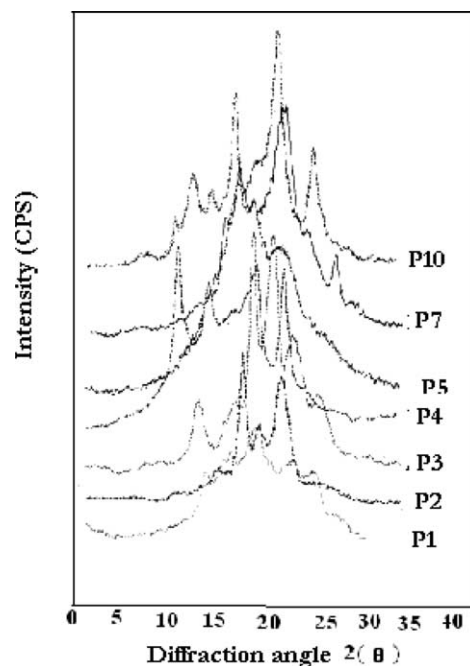


Fig. 7. WAXD pattern of (1) P1, (2) P2, (3) P3, (4) P4, (5) P5, (6) P7, (7) P10.

Table 5
Percentage of crystallinity

Sample	% of crystallinity
P1	40
P2	38
P3	45
P4	50
P5	54
P6	34
P7	46
P8	40
P9	42
P10	50
P11	39
P12	45

4. Conclusions

Hydrogen-bonded LC PEAs containing different structural moieties were synthesized and characterized for both thermotropic and lyotropic phase behaviors. It has been observed that the type of the structural units present in the polymer chain influenced the nature and extent of hydrogen bonding which in turn affected the chain stiffness and the persistence length. Incorporation of aromatic units in the PEAs exerted profound influence on the solubility, inherent viscosity, thermotropic and lyotropic behavior and also on the thermal stability. X-ray diffraction and FTIR spectral studies at different temperatures showed that hydrogen bonding and mesogenic interaction are greatly influenced by the structure and position of the aromatic moieties. X-ray diffractogram of PEAs showed that intermolecular hydrogen bonds are more or less perpendicular to the main chain direction, which induced the formation and stabilization of LC property in these PEAs. The ester segments can exist in more than one conformational form and hence it exhibits the transition from one smectic texture to another of the same texture. The mesogenic interaction is inter-plane interaction and hydrogen bonding is due to the in-plane interactions among the adjacent chains and thus, the rigidity due to aromatic structures coupled with the hydrogen bonding is responsible for the liquid crystallinity for the PEAs.

References

- [1] Constantinos M, Palcos M, Dimitris T. *Liq Cryst* 2001;28:1127.
- [2] Kato T. In: Demus D, Goodby GW, Gray HW, Spiess HW, Vill V, editors. *Hand book of liquid crystals*. Weinheim: Wiley; 1998.
- [3] Aharoni SM. *Macromolecules* 1988;21:1941.
- [4] Aharoni SM. *Macromolecules* 1989;22:686.
- [5] Fu-Sen Y, Leih-Li L, Jin-Long H. *Macromolecules* 1999;32:3068.
- [6] Murthy NS, Aharoni SM. *Macromolecules* 1992;25:1177.
- [7] Sudha JD. *J Polym Sci, Polym Chem* 2000;38:2469.
- [8] Sudha JD, Pillai CKS. *J Polym Sci, Polym Chem* 2003;41:335.
- [9] Sudha JD, Pillai CKS, Bera S. *J Polym Mater* 1996;13:317.
- [10] Sudha JD, Ramamohan TR, Pillai CKS, Schariah KJ. *Eur Polym J* 1999;35:1637.
- [11] Sudha JD, Pillai CKS, Bera S. In: Bhardwaj IS, editor. *Polymer science. Recent development edition*. New Delhi: Allied Publishers; 1994. p. 424.
- [12] Sudha JD, Pillai CKS. In: Venketachalam S, Joseph VC, Ramaswamy R, Krishnamoorthy VN, editors. *Macromolecules current trends edition*. New Delhi: Allied Publishers; 1995. p. 557.
- [13] Sudha JD, Menon ARR, Brahmakumar M, Pillai CKS. In: Anup G, editor. *International symposium on polymers beyond 2000*. India: Society for Polymer Science; 1999. p. 599.
- [14] Lee JB, Kato T, Yoshida T, Uryu T. *Macromolecules* 1995;28:2165.
- [15] Kosaka Y, Kato T, Uryu T. *Macromolecules* 1994;27:2658.
- [16] Qincui G, Shouxi C, Young H. *Polymer* 2004;43:2417.
- [17] Perrin DD, Armarego WLP. *Purification of laboratory chemicals*. Oxford: Pergamon Press; 1988. p. 26.
- [18] Sorensen WR, Campbell TW. *Preparative methods in polymer chemistry*. 2nd ed. New York: Interscience; 1968. p. 95.
- [19] Morgan PW. *Condensation polymers by interfacial solution method*. New York: Interscience; 1965. p. 103.
- [20] Van Krevelen DW. *Properties of polymers*. 2nd ed. New York: Elsevier; 1970.
- [21] Leipertz A, Spickermann M. In: Shrader B, editor. *Infra red and Raman spectroscopy*. Weinheim: VCH; 1995. p. 645–8.
- [22] Coleman MM, Shrovanek DJ, Hsu J, Painter PC. *Macromolecules* 1988;21:59.
- [23] Dana G, Howard W, Starkweather JR. *J Polym Sci, Polym Chem* 1985;23:537.
- [24] Haberkorn H, Illers KH, Simak P. *Colloid Polym Sci* 1979;25:870.
- [25] Uwe B. *Prog Polym Sci* 2003;28:1049.
- [26] Antonova K, Petrov M, Kirov N, Tenev T, Ratajczak H, Baran J. *J Mol Struct* 1994;325:189.
- [27] Nakamoto K, Markoshes M, Rudle R. *J Am Chem Soc* 1955;77:6480.
- [28] Krigbaum WR, Hakemi H, Kote R. *Macromolecules* 1984;18:965.
- [29] Bozena K, Danuta S. *Polymer* 1995;36:5019.
- [30] Bhowmic PK, Atkin EDT, Lenz RW. *Macromolecules* 1993;26:440.
- [31] Rubig C, Samuski ET. *Macromolecules* 1992;25:563.
- [32] Field ND, Baldwi R, Laytin R, Frayer, Scardiglia F. *Macromolecules* 1988;21:2155.
- [33] Kalika DS, Yoon DY, Inanelli P, Parrish W. *Macromolecules* 1991; 24:3413.
- [34] Ruan J, Ge JJ, Zhang AQ, Shi J. *Macromolecules* 2000;35:736.
- [35] Hui T, Jin-Cheri S, Kosaku O, Kaname K, Takashi K, Toshiyuri U. *J Polym Sci, Polym Chem* 1996;34:3407.
- [36] Anne KST, Clair, Norman JJ, Nasa-Langley. *J Polym Sci, Polym Chem Ed* 1977;15:3009.
- [37] East AJ, Charbenneau LF, Calundann GW. *Mol Cryst Liq Cryst Liq Cryst Ins Non-lin Opt* 1988;157:615.
- [38] Arnold H, Sackman HZ. *Phys Chem* 1987;137:145.
- [39] Tadokoro H. *Structure of crystalline polymers*. New York: Wiley; 1979.
- [40] Rubig C, Edward T, Samulski ET. *Macromolecules* 1994;27:135.
- [41] Bstiansen S, Sandal J. *Mol Struct* 1985;128:115.
- [42] Ruan J, Ge JJ, Zhang AQ, Shi J. *Macromolecules* 2002;35:736.
- [43] Black well J, Cheng HM, Biswas A. *Macromolecules* 1988;39:2155.
- [44] Taylor TR, Ferguson JL, Arora SL. *Phys Rev Lett* 1970;24:359.
- [45] Devries A. *J Chem Phys* 1974;61:15.